A Dual Pathway Heterogeneous Flow through Snow Model

NICOLAS R. LEROUX[1] AND JOHN W. POMEROY[2]

ABSTRACT

Accurate estimation of snowmelt flux is of primary importance for runoff prediction, which is used for water management and flood forecasting. Lateral flows and preferential flow pathways in porous media flow have proven critical for improving soil and groundwater flow models, but though many physically-based layered snowmelt models have been developed, only 1D matrix flow is accounted for in snow models. Therefore, there is a need for snowmelt models that include these processes so as to examine the potential to improve snowmelt discharge timing and contributing area in hydrological modelling. An initial dual pathway version of a two-dimensional snow model is presented that simulates vertical and lateral water flows through the snow matrix and preferential flow paths, internal energy fluxes, melt, and refreezing. The dual pathway model utilizes an explicit finite volume method to solve for the energy and water flux equations over an orthogonal grid. Energy available at the snow surface, and soil slope angle are set as model inputs. The initial conditions include the number of snow layer, their properties, temperatures, and liquid water contents. This heterogeneous flow model is an important tool to help understand snowmelt flow processes in complex and level terrains and how snowmelt-derived runoff forecasting might be improved.

Keywords: snowmelt, preferential flow paths, two-dimensional snow model, heat and mass transfers

 INTRODUCTION

   To accurately predict the timing and magnitude of snowmelt runoff from deep snowpacks, water flow percolation within snow must be understood (Gray and Male, 1975; Wankiewicz, 1979). Liquid water flow within the snowpack is influenced by the internal properties of the snowpack. Deeper, colder snowpacks have slower flow rates; this lag and attenuation in timing of meltwater delivery to the soil surface makes the process important for runoff and streamflow generation in mountains. Amongst the snowpack's internal properties, ice layers and flow fingers greatly impact the spatial and temporal distributions of snowmelt runoff (Marsh and Woo, 1984a; Marsh, 1991). Many theories have arisen to describe gravitational vertical flow percolation within a homogeneous, isothermal snowpack (Colbeck, 1972), water percolation through a subfreezing, layered snowpack with phase change (Illangasekare et al., 1990), or the influence of capillary forces on the water flow (Jordan, 1995).

[1] Centre for Hydrology, University of Saskatchewan, Saskatoon, SK, Canada
(nicolas.leroux@usask.ca)
2 Centre for Hydrology, University of Saskatchewan, Saskatoon, SK, Canada
(john.pomeroy@usask.ca)

Several numerical snowmelt models of differing levels of complexity have been developed in the past decades. Tseng et al. (1994) developed a complex two-dimensional snow model based on the theory of Illangasekare et al. (1990), but this theory has not been validated against *in-situ* data and does not incorporate preferential flow paths. Marsh and Woo (1985) created a one-dimensional model that assumed mass flow through different flow pathways; however, this theory does not include lateral flows, the delay of water flow due to ice layers and assumed that each flow path extends over the complete depth of the snowpack. No operational snow model in hydrological models or land surface schemes is able to predict lateral flows, the formation of flow fingers and ice layers and their effects on the water flow through snow, resulting in inaccuracy in the prediction of catchment discharge and meltwater delivery to soil (Pomeroy et al., 1998). Therefore, in this paper a novel two-dimensional snowmelt model solving for the mass and energy flows is presented. The model includes an implementation of the theory of Hirashima et al. (2014) to simulate the formation of preferential flow paths. The importance of the parameterization of the water entry pressure for dry snow and lateral heterogeneities in snow grain size and density are demonstrated.

MATHEMATICAL MODEL

Snowpack ablation and melt

A melting snow surface is a moving boundary at which heat transfer and phase change occur simultaneously. To estimate the heat transfer and phase change at this moving boundary, the Stefan condition is solved (Eq. 1) (e.g. Tseng et al., 1994).

$$Q_n = -\lambda \frac{\partial T}{\partial z}(z = S) + L_f \rho_s V_n \qquad \text{Eq. 1}$$

where

$$Q_n = -\lambda \frac{\partial T}{\partial z}(z = S) \qquad \text{if } T_s < 0^\circ\text{C}$$

$$Q_n = L_f \rho_s V_n \qquad \text{if } T_s = 0^\circ\text{C}$$

and Q_n is the heat flux at the surface [W/m^2], λ is the thermal conductivity [W/(K m)], $\partial T/\partial z$ the vertical temperature gradient at the surface [K/m], L_f the latent heat of fusion of ice [J/kg], ρ_s the snow density [kg/m^3], V_n the velocity of the melting snow surface [m/s], and T_s is the snow surface temperature [$^\circ$C].

The infiltration rate (Eq. 2) can be estimated from the vertical velocity of the melting snow surface V_n.

$$Q_{inf} = V_n(\frac{\rho_s}{\rho_w} + \theta) \qquad \text{Eq. 2}$$

where Q_{inf} is the infiltration rate at the snow surface [m/s], ρ_w the density of water [kg/m^3] and θ is the volumetric liquid water content within the melting volume. This infiltration rate, estimated from the energy available at the surface of the snowpack, is then used as a boundary condition for the water flow equations.

Water Flow

The mass flow between each snow layer is estimated by solving for the two-dimensional Richards equation (Eq. 3).

$$\frac{\partial \theta}{\partial t} + \nabla \vec{q} = S_s \qquad \text{Eq. 3}$$

4

where θ is the volumetric liquid water content, q is the macroscopic flow velocity [m/s] (Eq. 4) and S_s is a mass sink term due to refreezing of liquid melt water in each layer [kg/m^3.s].

The macroscopic flow velocity in an unsaturated medium is commonly estimated from Darcy's law under the condition that the flow is laminar (Reynolds Number < 1).

$$\vec{q} = K(\theta)\,\vec{\nabla}(\Psi(\theta) + z) \qquad \text{Eq. 4}$$

where $K(\theta)$ is the unsaturated hydraulic conductivity [m/s] and $\Psi(\theta)$ is the matric suction [m]. For unsaturated porous media, both are functions of the water content.

In snow science, studies have been conducted to establish relationships between snow hydraulic properties and water content. Calonne et al. (2012) developed a relationship between saturated hydraulic conductivity (K_s), dry snow density, and optical grain size (Eq. 5) through three-dimensional numerical computations. Knowing the saturated hydraulic conductivity, the unsaturated hydraulic conductivity can be estimated (e.g. Colbeck and Davidson, 1973) as,

$$K_s = 3\frac{\rho_w g}{\mu_w} r^2 \exp(-0.013\rho_{ds}) \qquad \text{Eq. 5}$$

with g the gravitational constant [m/s^2], μ_w the dynamic viscosity of water [Pa.s], r the optical grain radius [m] and ρ_{ds} the dry snow density [kg/m^3].

Snow water retention curves

The Water Retention Curve (WRC) is the relationship between matrix head and liquid water content. Analogous to flow through unsaturated soil, the snow WRC (Fig. 1) has hysteretic behaviour (Adachi et al., 2012). Yamaguchi et al. (2012) developed a WRC for snow based on the van Genuchten model (Eq. 6). Through laboratory experiments, they found empirical equations to link the parameters α and n (cf. Eq. 6) with dry snow density and optical grain size (Eq. 7). However, this WRC was developed only for drying snow, i.e. the snow was initially wet and liquid water was draining from it.

$$S_e = (1 - |\alpha\Psi|^n)^{-m} \qquad \text{Eq. 6}$$

where S_e is the effective saturation ($S_e = (\theta - \Phi)/(\theta_i - \Phi)$, with Φ the snow porosity and θ_i the irreducible water content), and α, n, and m are parameters (Eq. 7), with m chosen as $m = 1 - 1/n$.

$$\alpha = 4.4 \times 10^6 \left(2\frac{\rho_{ds}}{r}\right)^{-0.98} \qquad \text{Eq. 7}$$

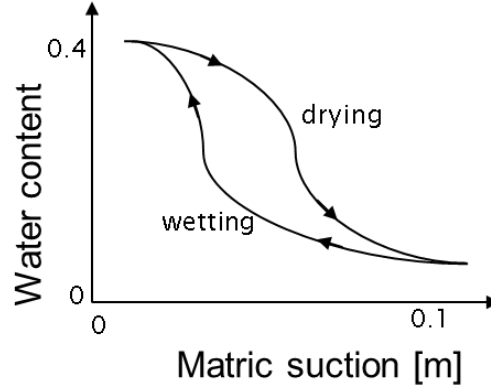$$n = 1 + 2.7 \times 10^{-3} \left(2\frac{\rho_{ds}}{r}\right)^{0.61}$$

Figure 1. Conceptual representation of the hysteretic behaviour between matric suction and liquid water content in the snow water retention curve.

However, in the case of wetting snow, i.e. snow that is initially dry and into which liquid water infiltrates, the model of Yamaguchi et al. (2012) is not applicable. Therefore, in the 2D model presented here, a new value of water entry pressure is taken from the study by Katsushima et al. (2013) when the initial water content of a cell is below the irreducible water content level (dry snow). The snow WRC developed by Yamaguchi et al. (2012) is used to estimate the matric head when the water content is above the irreducible water content (wet snow).

Implementation of a water entry pressure for wetting snow in a snow model

The impact of implementing a new water entry pressure for dry snow is presented through an example analyzing flow through two different snow layers. The upper layer (layer 1, a wet dense snow layer) has a dry density of 350 kg/m³ and an optical grain diameter of 0.3 mm. The lower layer (layer 2, a dry ice layer) has a density of 450 kg/m³ and an optical grain diameter of 0.7 mm (Figure 2).
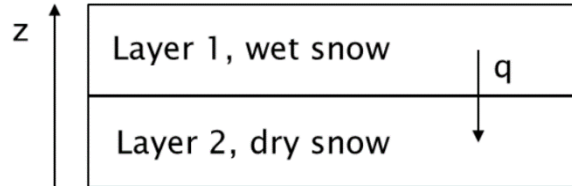

Figure 2. Representation of the two snow layers

The flux q between layer 1 and layer 2 was analyzed for two different cases:
- Variable water entry pressure: the model by Yamaguchi et al. (2012) is used for the upper wet snow layer and the Katsushima et al. (2013) water entry pressure is used for the lower dry snow layer.
- Wet water entry pressure: the model by Yamaguchi et al. (2012) is used for both dry and wet snow layers.

The flux q from layer 1 to layer 2 can be estimated using Darcy's law (Eq. 4) and liquid water flows from layer 1 to layer 2 only when q is positive.

Figure 3 shows the change of q/K with liquid water content in layer 1 for the two different cases considered. It can be observed that introducing a new water entry pressure for dry snow allows much more liquid water to accumulate in layer 1 before initiating downward flow and that this has the potential to simulate the ponding of liquid water at snow layer interfaces that is observed in nature.
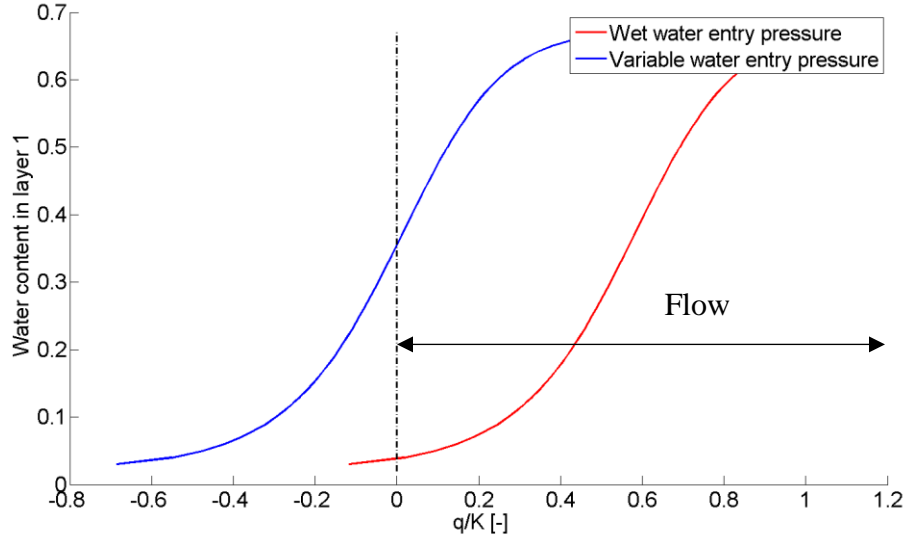
6

Figure 3. Change of liquid water in layer 1 with q/K

Implementation of snow heterogeneities

In their theoretical study on the triggering of preferential flow path formation, Hirashima et al. (2014) suggested these are due to spatial heterogeneities in snow grain size. The impact of adding a perturbation in snow grain size on the water flow is therefore discussed. Using the previous modelling example (Fig. 2), three cases are considered: i) the grain size in layer 2 is unchanged, ii) it is decreased by 1% and iii) it is increased by 1%. Figure 4 shows the water content in layer 1 as function of the flux q/K for the three different grain sizes in layer 2. It can be observed that greater water flow from layer 1 to layer 2 occur when there is a smaller grain size in layer 2: for this case the downward flux becomes positive at lower water contents in layer 1.
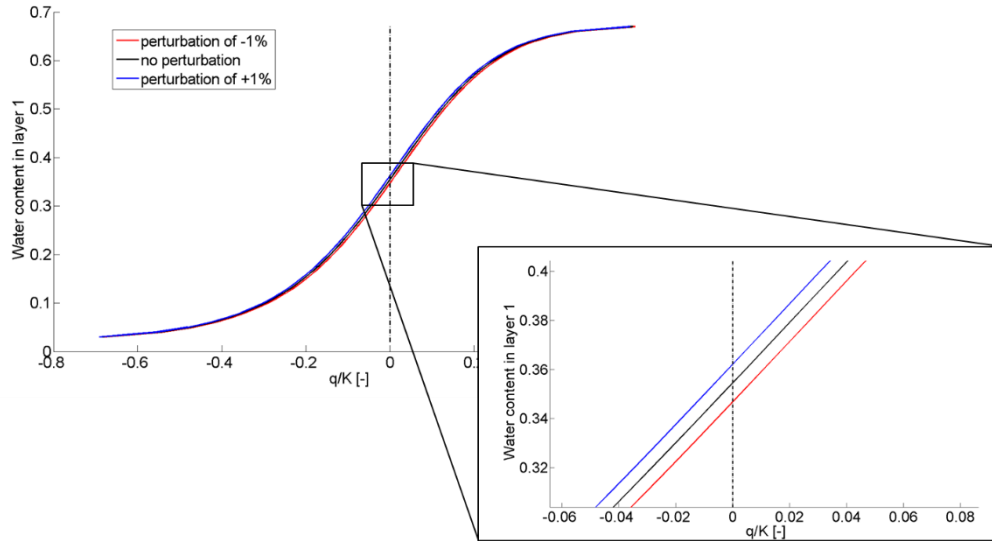

Figure 4. Change in the ratio q/K for different three grain sizes in layer 2

7

Refreezing of liquid water

In a wet subfreezing snowpack, heat and momentum transfers occur between the flowing liquid water and the solid phase. Illangasekare et al. (1990) developed a theory describing refreezing of meltwater in a subfreezing snowpack. They expressed the maximum mass of liquid water per unit volume of snow (m_{max}) that must freeze to raise the snow temperature to zero, i.e. to raise the snow cold content to zero (Eq. 8) as,

$$L_f m_{max} = -\rho_s C_{p,i} T \qquad \text{Eq. 8}$$

where T is the temperature of snow layer [K] and $C_{p,i}$ is the specific heat capacity of ice [J/(kg K)].

However, the real mass of liquid water per unit volume of snow that refreezes during a numerical time step (m_f) is always less than or equal to m_{max}, as m_f is limited by the available liquid water content in the snow layer. The new snow layer temperature at the end of a numerical time step Δt can then be estimated using Eq. 9.

$$T^{t+\Delta t} = \frac{\rho_s^t C_{pi} T^t + m_f L_f}{\rho_s^{t+\Delta t} C_{pi}} \qquad \text{Eq. 9}$$

At the end of the same time step, snow porosity (ϕ), effective water saturation (S_e), and snow density (ρ_s) are also updated as shown in Eq. 10:

$$\Phi^{t+\Delta t} = \Phi^t + \frac{m_f}{\rho_i} \qquad \text{Eq. 10}$$

$$S_e^{t+\Delta t} = \frac{\theta^t - m_f/\rho_w}{\Phi^{t+\Delta t}}$$

$$\rho_s^{t+\Delta t} = \rho_s + m_f \qquad .$$

Heat transfers in snow

To simulate heat transfers in the snowpack, the two-dimensional heat conduction equation is solved following Albert and McGilvary (1992):

$$\left(\rho C_p\right)_s \frac{\partial T}{\partial t} = \frac{\partial}{\partial x_k}\left(\lambda \frac{\partial T}{\partial x_k}\right) \quad \text{with } k{=}1,2 \text{ representing the two spatial directions} \qquad \text{Eq. 11}$$

such that $\left(\rho C_p\right)_s = \left(\rho_a \theta_a C_{p,a}\right) + \left(\rho_w \theta_w C_{p,w}\right) + \left(\rho_i \theta_i C_{p,i}\right)$

where T is the temperature of a snow layer [K], ρ the density [kg/m³], C_p the specific heat capacity [J/(K kg)], and θ the fractional volumetric of each component. The subscripts a, w, i and represent each component of the snowpack: air, water, and ice.

Calonne et al. (2011) conducted three-dimensional numerical computations of snow conductivity through the air and ice phases. They developed an empirical relationship between the thermal conductivity and the dry snow density:

$$\lambda = 2.5\text{x}10^{-6}\, \rho_{ds}^2 - 1.23\text{x}10^{-4} \rho_{ds} + 0.024 \qquad \text{Eq. 12}$$

NUMERICAL MODEL DESIGN

A two-dimensional numerical snow model based on the snow physics presented above was developed to solve for the heat and mass fluxes within a two-dimensional heterogeneous, layered, subfreezing snowpack. To solve for the partial differential equations, an explicit finite-volume scheme was used over an orthogonal structured mesh (Fig. 5). This method considers each numerical cell as a control volume, in which the conservation equations are solved. This approach is commonly applied in computational fluid dynamics models, as it is inherently conservative.

Boundary and initial conditions

Neumann boundary conditions were applied at the upper and left-hand boundaries for the mass and heat equations. At the upper boundary, a constant heat flux (Q_n in Eq. 1) was applied as boundary condition for the heat equation. This flux is then used to estimate the infiltration rate utilized as upper boundary condition for the mass flow equation. The left-hand boundary condition is a no-flow condition, whereas the lower and right-hand boundary conditions are set as free boundary conditions, i.e. water was allowed to drain through these two boundaries by gravity flow.

The snowpack and its properties were initialized before running the model. These data include the snowpack slope angle (γ in Fig. 5), the snowpack layering system and the mean layer properties − mean porosities, water contents, mean optical grain sizes, and temperatures. A random lateral perturbation was added to each snow layer density and optical grain size. This perturbation is less or equal to 1% of the mean density and optical grain size values. Also, a new water entry pressure was used for dry snow.

Model assumptions

Water and energy flows within a layered, heterogeneous, subfreezing snowpack are very complex physical processes. Therefore, due to the lack of complete understanding of the physics of these processes, it is necessary to make assumptions while developing a numerical snow model. The assumptions made in this model also indicate current knowledge and how this limits snow melt modelling of water flow through snow. These assumptions are:

1. The change of grain size due to temperature gradient and presence of liquid water is not simulated.
2. The irreducible water content is assumed constant for the whole snowpack and does not depend on the snow properties.
3. Thermal convection, condensation, and sublimation within the snowpack are not simulated.
4. Heat conduction dominates the heat transfers.
5. Freezing point depression effects on snow grains is neglected.
6. The lateral heterogeneities in snow grain size and density are randomly distributed over space.
7. The water entry pressure for dry snow is function only of snow grain size.
8. Temperature, density, and water content are computed at the centre point of each cell and are assumed homogeneous within the cell.
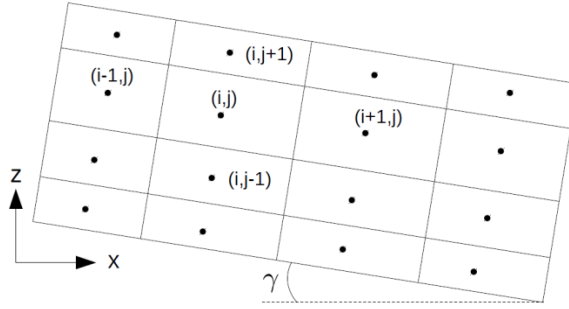
Figure 5. Mesh used to represent a layered sloping snowpack

MODEL APPLICATIONS

A first model simulation of water and heat flow through a subfreezing, heterogeneous, layered snowpack is demonstrated. The snowpack was divided into four horizontal snow layers (Table 2, Fig. 6). The third layer (from the bottom of the snowpack) is an ice layer with a higher density than the other layers. Under natural conditions, flowing liquid water accumulates over this layer and preferential flow paths were observed to form below a saturated horizontal layer (Marsh and Woo, 1984a).

Table 1 summarizes the parameters and inputs used in the model as initial and boundary conditions, and Table 2 shows the snow layering properties. The values used for the mean optical grain sizes in Table 2 were computed from the average specific surface areas measured by Montpetit et al. (2012) for different types of snow.

The simulation was run until the snowpack completely melted. Figures 7 and 8 show the water content within the snow matrix layers after 2 h 45 min and 4 h 10 min of melt, respectively. It can be observed that liquid water accumulates above the ice layer (Fig.7). Then, as liquid water accumulates above this layer, preferential flows occur where the grain size in the ice layer is smaller due to the perturbation implemented (Fig. 8) (cf. section *Implementation of snow heterogeneities*).
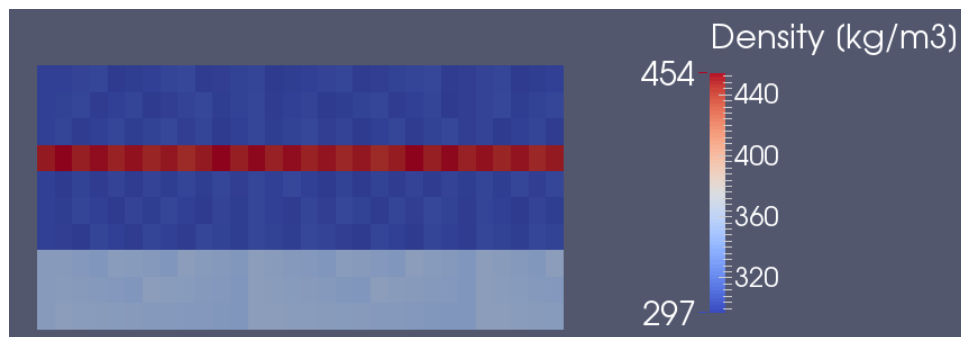

Figure 6. Initial density in each snow layers

10

Table 1. Inputs used for the simulation

Horizontal length of snowpack	2 m
Snow depth	1 m
Number of horizontal layers	30
Number of vertical layers	10
Ground slope angle	0
Temperature at the interface snow-soil	0°C
Energy at the surface	500 W/m^2
Irreducible water content	0.02

Table 2. Snow matrix properties

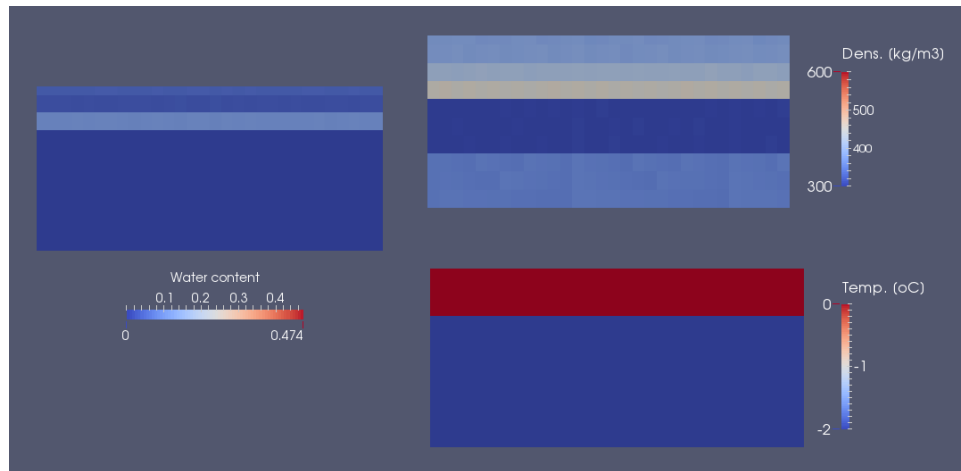|	Type of snow	Thickness [m]	Temperature [^{o}C]	Density [kg/m^3]	Optical grain diameter [mm]
Layer 1 (bottom)	Coarse depth hoar	0.3	-2	350	0.5
Layer 2	Dense rounded snow	0.3	-2	300	0.3
Layer 3	Ice layer	0.1	-2	450	0.7
Layer 4	Fresh snow	0.3	-2	300	0.3

Figure 7. Water content, density and temperature distributions in the snowpack after 2 h 45 min of melt
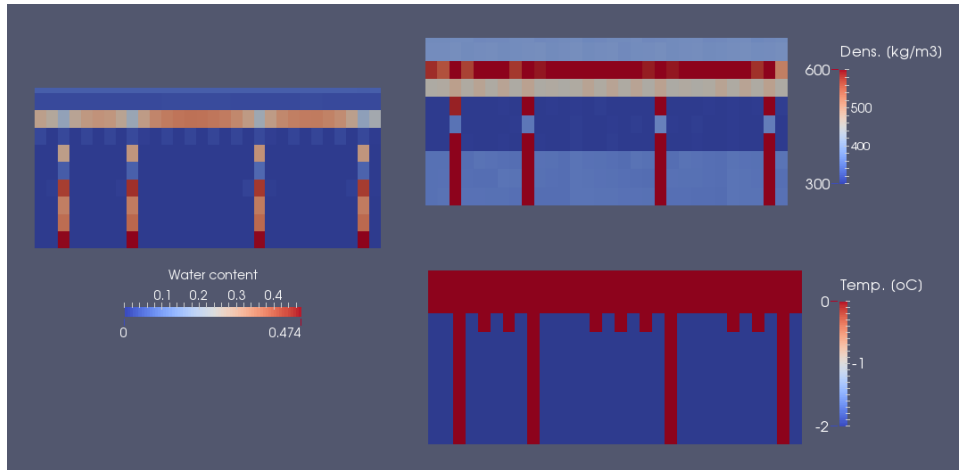
Figure 8. Water content, density and temperature distributions in the snowpack after 4 h 10 min of melt

A second model application of water flow through a sloping snowpack is also demonstrated. The same initial conditions are applied as before, but the snowpack is now tilted by 5°. Figures 9 and 10 show the water content in the sloping snowpack after 1 h 45 min and 1 h 50 min of melt, respectively. It is observed that preferential flows form in the downhill section of the snowpack (Fig. 9) as higher water content occurs in this area due to lateral flows above the ice layer. After the formation of preferential flow paths, liquid water flows laterally (Fig. 10).
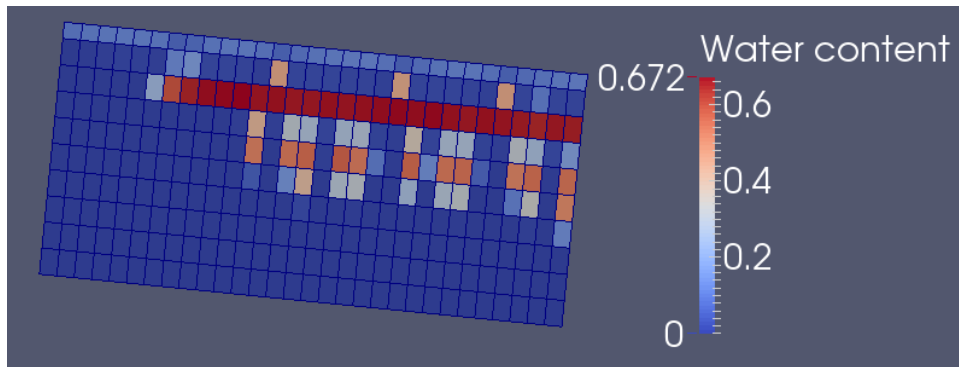

Figure 9. Water content in a sloping snowpack after 1 h 45 min of melt
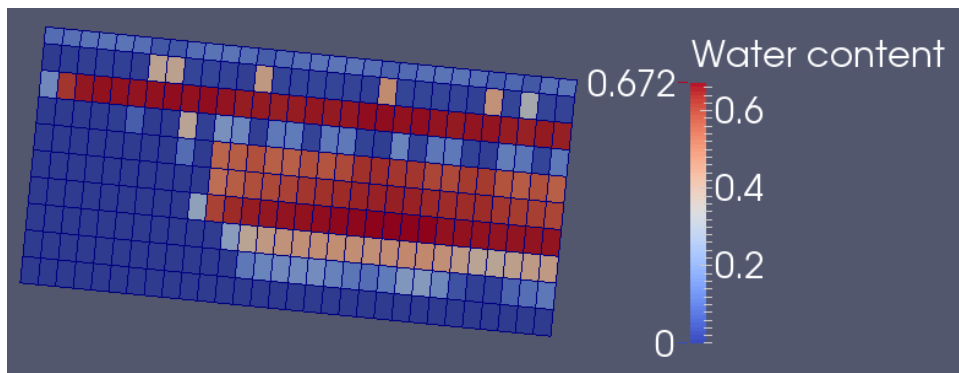

Figure 10. Water content in a sloping snowpack after 1 h 50 min of melt

12

CONCLUSIONS

A first attempt to model mass and energy flows through a subfreezing, layered, sloping snowpack with preferential flow path formation has been demonstrated. Two parameters have been introduced and explored for their role in triggering the formation of preferential flows – a water entry pressure for dry snow and a perturbation in snow grain size and density to simulate lateral heterogeneities in their properties. In the model applications presented here, the spatial distributions of the perturbations were random. Therefore, further work should be carried to establish relationships between these parameters and snow matrix properties from field observations.

This two-dimensional snow model needs to be validated against *in-situ* data. A field study is being designed to validate each physical process simulated by the model. The development of this numerical model raises questions on water flow through snow and numerical snow modelling:

1. Does the irreducible water content depend on snow properties?
2. How should the hydraulic conductivity and thermal conductivity be numerically computed at the interface of two numerical nodes?
3. How should grain size and density perturbations be represented?
4. How should the water entry pressure for dry snow be related to snow density?
5. Does all the available liquid water that can refreeze (m_{max}) do so during a numerical time step (Illangasekare et al., 1990)?
6. Is the flow through preferential flow paths laminar? Does Darcy's law always apply?
7. Can the equation used for the thermal conductivity in a dry snowpack (Eq. 12) be used when liquid water content is present within the snowpack?
8. Does liquid water refreeze at $0^{o}C$ or is there a freezing point depression that depends on snow properties and surface tension between ice and liquid water?

ACKNOWLEDGEMENTS

REFERENCES

Adachi S., Yamaguchi S., Ozeki T., and Kose K. 2012. Hysteresis in the water retention curve of snow measured used an MRI system, *ISSW Proceedings 2012*, *Anchorage, Alaska,* 918-922.

Albert M. and McGilvary W. 1992. Thermal effects due to air flow and vapor transport in dry snow. *Journal of Glaciology* **38**(129): 273–281.

Calonne N., Geindreau C., Flin F., Morin S., Lesaffre B., Rolland Du Roscoat S., and Charrier P. 2012. 3-D image-based numerical computations of snow permeability: links to specific surface area, density, and microstructural anisotropy. *The Cryosphere* **6**: 939–951.

Colbeck S. 1972. A theory of water percolation in snow. *Journal of glaciology*, 11(63), 369–385.

Colbeck S. and Davidson, G. 1973. Water percolation through homogeneous snow. *Proceedings, the Role of Snow and Ice in Hydrology* **4:** 242–257.

Gray D. M. and Male D. H. 1975. Problems in developing a Physically Based Snowmelt Model. *Canadian Journal of Civil Engineering* **2**(4): 474–488.

Hirashima H., Yamaguchi S., and Katsushima T. 2014. A multi-dimensional water transport model to reproduce preferential flow in the snowpack, *Cold Regions Science and Technology* **108**: 80-90

Illangasekare T. H., Walter R. J., Meier M. F., and Pfeffer W. T. 1990. Modeling of meltwater infiltration in subfreezing snow. *Water Resources Research* **26**(5): 1001–1012.

Jordan R. 1995. Effects of capillary discontinuities on water flow and water retention in layered snowcovers. *Defence Science Journal* **45**(2): 79–91.

Katsushima T., Yamaguchi S., Kumakura T., and Sato A. 2013. Experimental analysis of preferential flow in dry snowpack, *Cold. Reg. Sci. Technol.* **85**: 206-216.

Marsh P. 1991. Water flux in melting snow covers. Chapter 2 in: M.Y. Corapcioglu (Editor). *Advances in porous media*, Vol. 1, Elsevier, Amsterdam, 61–124.

Marsh P. and Woo M. 1984. Wetting front advance and freezing of meltwater within a snow cover: 1. Observations in the Canadian Arctic. *Water Resources Research* **20**(12): 1853–1864.

Marsh P. and Woo M. 1985. Meltwater movement in natural heterogeneous snow covers. *Water Resources Research* **21**(11): 1710–1716.

Montpetit B., Royer A., Langlois A., Cliche P., Roy A., Champollion N., Picard G., Domine F., and Obbard R. 2012. New shortwave infrared albedo measurements for snow specific surface area retrieval, *Journal of Hydrology* **58**(211): 941-952.

Pomeroy J.W., Gray D.M., Shook K.R., Toth B., Essery R.L.H., Pietroniro A., and Hedstrom N.R. 1998. An evaluation of snow accumulation and ablation processes for land surface modelling, *Hydrological Processes* **12**: 2339-2367

Tseng P., Illangesakare T., and Meier M. 1994. Modeling of snow melting and uniform wetting front migration in a layered subfreezing snowpack. *Water Resources Research* **30**(8): 2363–2376.

Yamaguchi S., Watanabe K., Katsushima T., Sato A., and Kumakura T. 2012. Dependence of the water retention curve of snow on snow characteristics. *Annals of Glaciology* **53**(61): 6–12.